



Semnan University



Two-dimensional Simulation of Mass Transfer and Nano-Particle Deposition of Cigarette Smoke in a Human Airway

Masoud Khajenoori, Ali Haghghi Asl*

Faculty of Chemical, Gas and Petroleum Engineering, Semnan University, Semnan, Iran

PAPER INFO

History:

Submitted: 2016-11-18

Revised: 2017-08-21

Accepted: 2017-10-29

Keywords:

Lung airway;
Cigarette smoke;
Nano-particle;
Mass transfers;
Deposition.

ABSTRACT

The chance of developing lung cancer is increased through being exposed to cigarette smoke illustrated by studies. It is vital to understand the development of particular histologic-type cancers regarding the deposition of carcinogenic particles, which are present in human airway. In this paper, the mass transfer and deposition of cigarette smoke, inside the human airway, are investigated applying the finite element method. The mass transfer and depositions of four types of critical cigarette smoke, namely 1, 3-butadiene, acrolein, acetaldehyde and carbon monoxide (CO), in a complete human-airway model (from mouth to B3 generation), under inhalation conditions, have been simulated. In this study, concentration distribution in inhalation is evaluated. The vapour deposition was modelled with 30 and 80 L.min⁻¹ volumetric flow rates. Therefore, a two-dimensional model of human airway from the mouth to generation B3 was reconstructed. Then, for simulating the mass transfers and deposition fraction, the low-Reynolds-number (LRN) $k-\omega$ turbulence equation was used.

© 2018 Published by Semnan University Press. All rights reserved.

DOI: 10.22075/jhmtr.2017.1503.1100

1. Introduction

Most likely, cigarette smoking is the toxic chemical-exposure in human only most important factor. By the year 2020, the World Health Organization predicts cigarette smoke will lead to killing of approximately 10 million people per year internationally [1]. More than 6000 compounds have been distinguished in cigarette smoke so far [2]; probably, at least 69 of which are known as carcinogens for humankind [3]. In addition, the food and drug administration (FDA) [4] listed cigarette smoke constituents which are potentially harmful. Smoking results in potential threat to the respiratory tract where roughly half of all cigarette smoking related health impacts materialize. Cigarette smoke is a complex mixture of gaseous compounds. Current literature shows 4800 known gases in cigarette smoke. Cigarette smoking is a complicated aggregation of

particulate phase and liquid droplets which suspend in a mixture of gases and vapors. The droplets range in different mean diameter ($dp < 100$ nm) [6] and the toxic agents are dissolved in both vapors and droplets [5]. Cigarette smoking leads to various kinds of illnesses such as primarily lung tumors and asthma, deficiencies of the respiratory organs [7]. Particularly, two potential deadly results are lung cancer and chronic obstructive pulmonary disease (COPD) [8]. Briefly, the most important carcinogens in cigarette smoke vapor compounds are such as acrolein; acetaldehyde; 1, 3-butadiene; benzene; carbon monoxide; cadmium; ethylene oxide; 4-aminobiphenyl; formaldehyde; N-nitrosornicotine (NNN); and 4 (methylnitrosamino)-1-(3-pyridyl)-1-butanone (NNK). Some of these toxicants (such as acrolein; 1, 3-butadiene; acetaldehyde; carbon monoxide) inhaled from cigarettes appear as gas/vapor. Thus, the mass transfer of such vapors and

* Corresponding Author: A. Haghghi Asl, Semnan University, Semnan, Iran.
Email: ahaghghi@semnan.ac.ir

deposition fraction in human lungs are directly relevant to the tobacco smoking harmful impact [9]. Moreover, since many inhaled toxic or drug aerosols could partially appear in the form of vapor, human airway validated computer simulation would provide essential data for health and safety modeling. The airflow velocity is often expressed by the Navier-Stokes equations [10]. Navier-Stokes equations have been solved via a complex numerical analysis. Nevertheless, they have been applying a lot nowadays. The reason is that there are a lot of high-performance computers nowadays. An analytical method is achievable to solve the Navier-Stokes equations in some particular conditions [11]. The previous studies have been developed via the turbulent models by some researches [12, 13]. These models were developed to assess the nano-particle distributions in the human airway [7, 14]. The finite element method of analysis have been done already to solve the computational model of heat and mass transfer for nano-particle water vapor of the upper human airway [15]. In this paper, a new model is used to simulate cigarette smoke flow in the total lung airway which consists of the mouth-to-generation B3 pathway (see Figure 1). Furthermore, some species of vital carcinogens in cigarette smoke vapor compounds as the kinds for gas/vapor transport/deposition researches: acrolein; 1, 3-butadiene; acetaldehyde and carbon monoxide. Therefore, they come out at the oral entrance in the gas phase [16]. Thus, this model predicts mass transfer and deposition of cigarette smoke in all over lung. The paper is structured as follows: provides the background information about two-dimensional geometric model of the total lung airway, illustrates the changes in velocity profile for mouth and trachea, describes the mass transfer in human airway and the deposition of nano-particles in the 1~100 nm diameter range, presents the particle deposition fractions under different flow rate and provides the distributions of local Sherwood number for cigarette smoke. The goal of the study was to provide a more accurate description of mainstream smoke properties in the human airway during smoking and the various influences that determine those properties. But, there is not any experimental data to evaluate the simulation results. The results of particle deposition in different flow rates are compared with those reported by Zhang and Kleinsrteuer [17]. Finally, the paper will draw some conclusions.

2. Methods

2.1 Background information

A key parameter to assess the effects of inhaled cigarette smoke is the particle deposition in lung airway. It is costly and arduous the comprehensive particle deposition characterization in the total (upper and lower) airway using experimental methods. Therefore, the particle motion numerical simulation in

the airway is an efficient method to confront with this problem, and it could indicate the patterns of particle deposition in the whole lung airway. The upper and lower airways are the divisions of the total lung. The model of airway includes of oral cavity (mouth and palate), pharynx, larynx, trachea, B1, B2 and B3. There are resemblance between the human airway model dimensions with a human cast reported by Zhang et al. [18]. As indicated in Figure 1, the glottis to the first carina length and the mouth to the trachea length were near to 14 and 12 cm, respectively [18-19]. Furthermore, 1.60 cm was the trachea diameter. In this model, the airway wall is presumed as smooth and rigid. The cartilaginous rings impacts are not considered appearing in the human airway.

2.2 Governing equations in human airway

In the total lung airway system, some doubts existed for the transition of turbulent flow on the flow rate critical Reynolds number. The approximation of turbulent flow for a flow rate more than $12 \text{ L}\cdot\text{min}^{-1}$ was reported by Moghadas, et al. seeming rational particularly for track and field as the vibrant activities [20-22]. The Navier-Stokes equations and the continuity equation are dominant equations for the oscillating two-dimensional airflow. Zhang and Kleinstreuer [10] illustrated that it is decent for such internal laminar-to-turbulent flows. Generally, the equations of transport in tensor notation shows indirectly the double-index summation convention [10].

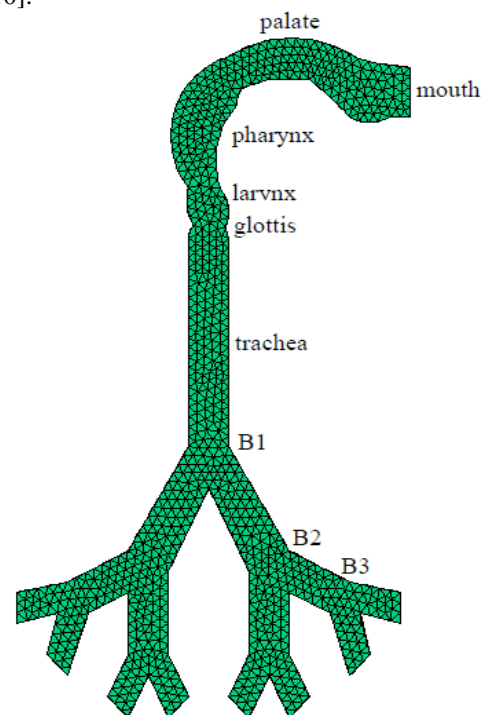


Figure 1. The model of airway based on the Zhang et al. model. [18, 7].

Continuity equation:

$$\frac{\partial u_i}{\partial x_i} = 0 \quad (1)$$

Momentum equation:

$$\frac{\partial u_i}{\partial t} + u_j \frac{\partial u_i}{\partial x_j} = -\frac{1}{\rho} \frac{\partial p}{\partial x_i} + \frac{\partial}{\partial x_j} \left[(v + \nu_T) \left(\frac{\partial u_i}{\partial x_j} + \frac{\partial u_j}{\partial x_i} \right) \right] \quad (2)$$

Turbulent kinetic energy (k) equation:

$$\frac{\partial k}{\partial t} + u_j \frac{\partial k}{\partial x_j} = \tau_{ij} \frac{\partial u_i}{\partial x_j} - \beta^* k \omega + \frac{\partial}{\partial x_j} \left[(v + \sigma_k \nu_T) \left(\frac{\partial k}{\partial x_j} \right) \right] \quad (3)$$

Pseudo-vorticity (ω) equation:

$$\frac{\partial \omega}{\partial t} + u_j \frac{\partial \omega}{\partial x_j} = \tau_{ij} \alpha \frac{\omega}{k} \frac{\partial u_i}{\partial x_j} - \beta \omega^2 + \frac{\partial}{\partial x_j} \left[(v + \sigma_\omega \nu_T) \left(\frac{\partial \omega}{\partial x_j} \right) \right] \quad (4)$$

For simplicity, summation sign is used with $i, j=1, 2$ where the x, y components of the velocity and the spatial coordinate vector are u_1, u_2 and x_1, x_2 , respectively. Time, density, pressure, kinetic molecular viscosity of the cigarette smoke, Reynolds stress tensor, turbulence kinetic energy, and dissipation per unit turbulence kinetic energy are the $t, \rho, p, \nu, \tau_{ij}, k$ and ω , respectively. The turbulent viscosity, ν_T is given as $\nu_T = k c_\mu f_\mu / \omega$, and the function f_μ is defined as $f_\mu = \exp[-3.4 / (1 + R_T / 50)^2]$ with $R_T = \rho k / (\omega \mu)$ while μ is the dynamic molecular viscosity ($\mu = \rho \nu$); $c_\mu, \alpha, \beta, \beta^*, \sigma_k$, and σ_ω are turbulence constants, i.e., $c_\mu = 0.09, \alpha = 0.555, \beta = 0.8333, \beta^* = 1, \sigma_k = \sigma_\omega = 0.5$.

The primary values in inlet of k and ω are calculated by [10]:

$$k_{in} = 1.5 (I \times P_{in}) , \quad \omega_{in} = \frac{k_p^{0.5}}{0.6 R} \quad (5)$$

Where the turbulence intensity and the radius of inlet tube are I and R , respectively. The convection–diffusion mass transfer equation of nano-particles, where the dominant transfer mechanisms are Brownian motion and turbulent dispersion, can be written as

$$\frac{\partial Y}{\partial t} + \frac{\partial}{\partial x_j} (u_j Y) = \frac{\partial}{\partial x} \left[\left(\tilde{D} + \frac{\nu_T}{\sigma_Y} \right) \frac{\partial Y}{\partial x_j} \right] \quad (6)$$

Where \tilde{D} is the molecular diffusivity of the cigarette smoke. The diffusivity in cigarette smoke is not very significant from compound to compound [17]. $Y_w=0$ is the boundary condition at the wall regarding that a perfect sink for aerosols or vapours upon touch is the airway wall. This idea is rational for fast gas-wall reaction kinetics, or vapours of high solubility and reactivity, as well as appropriate for estimating the maximum deposition of vapours in the airways. The aerosol diffusion coefficient is calculated as follows [23, 24]:

$$\tilde{D}_p = \frac{(k_B T C_{slip})}{(3\pi \mu d_p)} \quad (7)$$

Where T is the cigarette smoke temperature, k_B is the Boltzmann constant ($1.38 \times 10^{-23} JK^{-1}$), d_p is the particle diameter and C_{slip} is the Cunningham slip correction factor [25]:

$$C_{slip} = 1 + \frac{2\lambda_m}{d_p} \left[1.142 + 0.058 \exp \left(-0.999 \frac{d_p}{2\lambda_m} \right) \right] \quad (8)$$

where λ_m is the air mean free path. The nano-particles local wall mass flux could be calculated as [10]

$$m_w = -\rho A_i \left(\tilde{D} + \frac{\nu_T}{\sigma_Y} \right) \frac{\partial Y}{\partial n} \Big|_i \quad (9)$$

Where the area of local wall cell (i) is A_i , and the direction normal to the wall is n . The local deposition fraction (DF) of nano-particles, defining as the ratio of local wall mass flux to the inlet mass flux, expressed as

$$DF_{local} = \left[-\rho A_i \left(\tilde{D} + \frac{\nu_T}{\sigma_Y} \right) \frac{\partial Y}{\partial n} \Big|_i \right] / (Q_{in} Y_{in}) \quad (10)$$

and the regional DF can be determined as

$$DF_{region} = \sum_{i=1}^{n_w} \left[-A_i \left(\tilde{D} + \frac{\nu_T}{\sigma_Y} \right) \frac{\partial Y}{\partial n} \Big|_i \right] / (Q_{in} Y_{in}) \quad (11)$$

Where the number of wall cells in one particular airway area is n_w , e.g., oral airway, first airway bifurcation, etc., as well as the flow rate and mass fraction at the mouth are Q_{in} and Y_{in} , respectively. The regional deposition fraction could be calculated based on the Fick's law [7]. The model are used for a range of flow rates from 30 L/min to 80 L/min, corresponding to inlet mean velocities of 0.9417 m/s to 2.354 m/s, particle inlet velocities from 5.1 m/s to 8.4 m/s, and varying particle diameters from 1 nm to 100 nm. $T_{wall} = 310$ K. Also boundary condition no slip at the wall and Pharynx and larynx wall are rigid.

3.1 Characteristics of velocity structures

Selected cross sections of the 1-2 models, Profile flows, in the mouth and trachea, are displayed in figures 2a that velocity is fully develop, and 2b figures show the velocity profile for mouth and trachea at an inhalation flow rate of 60 L/min. The glottis, one of the cross-sectional areas is less than other ones of the human airway. Thus, the difference of cross-sectional areas results in the resistance against increment in various flow rates. This resistance created against the air flow decreases the mean velocity. As shown in theses figures, the central part of velocity profile is higher than the edges. The velocity of flow varies from a minimum on walls to a maximum in mouth and trachea section.

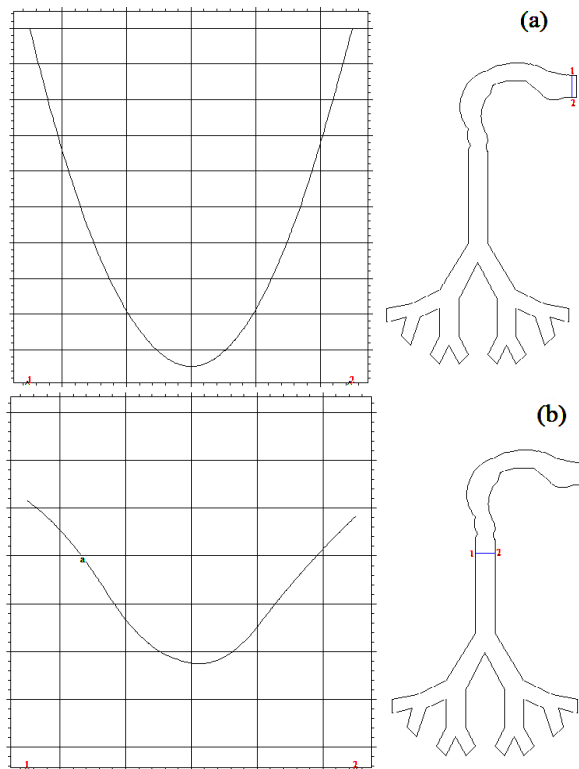


Fig. 2. The changes velocity profile for (a) mouth and (b) trachea inhalation flow rate of 60 L/min

3.2 Nano-particle deposition

The deposition fraction versus the nano-particle diameters for different rates of cigarette smoking is depicted in the Figure 3. As shown, the deposition of particle decreases with the diameter increment. The concentration of particle in cigarette smoke is totally high ($\sim 10^{12}$ particles in one cigarette). Moreover, the hygroscopic nature of the smoke droplets leads to rapid changes in diameter of particle through condensation and coagulation [26]. Gravitational sedimentation, inertial impaction and Brownian motion (diffusion) are the three basic mechanisms that influence on the behaviour of particles in cigarette smoke within the respiratory tract. ‘Aerodynamic’ effects such as sedimentation and impaction are the important ones. They increase with size increment. Although aerodynamic impacts are negligible for particles of significantly small size, thermodynamic effects are negligible for large particles. The smoke particle deposition lies on the particle size which may vary because of the high relative-humidity condition in the respiratory tract. Although the diameter of the smoke particles is small, 60–80% efficiencies of smoke deposition in the lung have been reported [27]. Upon the high flow rate, the nano-particles are interlocked. Because of the weight increment, they deposit on airway walls. Thus, through flow rate increment, the deposition of particle decreases. Accordingly, the inhalation of cigarette smoke nano-particles in low-flow rate could results in more damage in the lung airway. The results of particle

deposition in different flow rate are in good agreement with the simulation results reported by Zang and Kleinsrteuer [17].

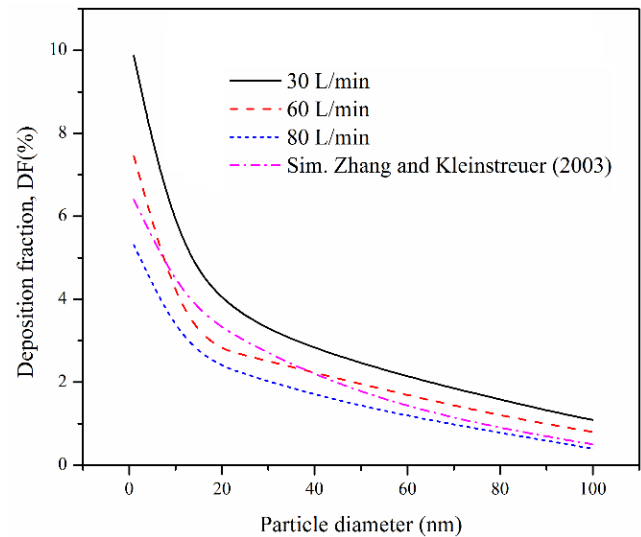


Fig. 3. Deposition fractions of particle under different flow rates

Figure 4 indicates the selected four vapour deposition fractions of cigarette smoke in the human airways, which incorporate the representative wall absorption conditions. In this case, steady puffing with inspiratory in different flow rates from 30 to 80 L/min. During puffing (3 sec), the soft palate (or glottis) is closed for most smokers; however, some smokers, directly, inhale the aerosols in to the lung [28]. In this study, steady puffing inhalation refers to the latter (presumably worst) case, so that the aerosols are assumed to be inhaled directly in to the lung. Clearly, the impact of airway wall absorption (or vapor solubility) can be vital for vapor deposition in human airways. The deposition fractions versus the diameter of nano-particle for various cigarette smoking rates are indicated in the Figure 3. As indicated, the deposition of particle decreases with the diameter increment. The nano-particles are interlocked under the flow rates of high values. Moreover, they deposit on walls of the airway because of the weight increment. On the other hand, the deposition of particle decreases with increasing the flow rate. Consequently, the inhalation of harmful nano-particles in the flow rates of low values could result in more damage in the lung airway. As shown in figure 4, the vapor deposition fraction butadiene vapor and carbon monoxide depositions are much lower than those of acrolein and acetaldehyde. Moreover, acrolein and acetaldehyde fully deposit in the upper airways of human from the mouth to generation B3. The deposition of butadiene vapor and carbon monoxide is very low in the upper airways. It is possible that the butadiene vapor and carbon monoxide depositions are much lower than those of acrolein and acetaldehyde.

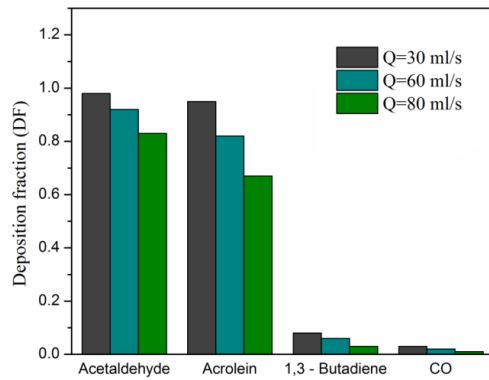


Fig.4. Vapor deposition fraction in the human airway

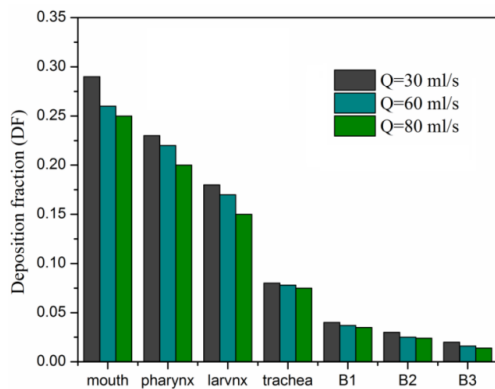


Fig.5. Vapour deposition fractions of the regions in the airway model

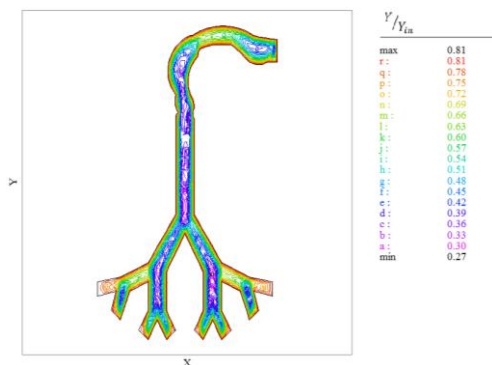


Fig. 6. The concentration distribution of nano-particles ($d_p = 5$ nm) in the airway model during cyclic inhalation for cigarette smoke vapors, rate: $Q_{in} = 60$ L/min, $Y_{in} = 0.8$.

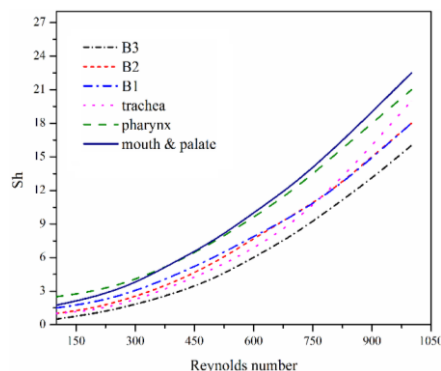


Fig.7. The changes of Sh number versus Re number.

The local deposition fractions (DFs) for vapors of acetaldehyde and acrolein are shown in Figure 5. The regional deposition for acrolein and acetaldehyde might gradually decrease from the cavity of mouth to bifurcation B3 because of the heavy deposition, leading to lower vapor concentrations at the each inlet of downstream regions. Furthermore, the different airway region surface areas lead to different values of vapor deposition. For instance, while Trachea has the lowest deposition, it receives the highest vapor deposition in the Larvnx. The different airway geometries, surface areas, local flow rates and concentrations of inlet vapor are influential and the deposition fractions in individual bifurcations vary as well. Carbon monoxide and butadiene vapor deposition is very low in the airway model from the oral cavity to generation B3.

The concentration distribution of nano-particles ($d_p = 5$ nm) in the upper airway model for the cigarette smoke vapors flow rate of 60 L/min during cyclic inhalation have been indicated in the figure 6. As indicated, the airway edges concentration profile is higher than airway center. Because of the less soluble vapors such as cigarette smoke the wall concentration would be greater than zero so that mass transport in center and in airways must be considered simultaneously when simulating vapor uptake. The most concentration distribution is in the palate, pharynx and larynx section. Because of the nano-particle deposition in the airway length, this distribution of concentration reduces slowly. The mass transfer occurs often in the mouth and palate (oral airway). Therefore, the inhalation of cigarette smoke vapors creates the more damage on the oral airway and B3 section.

The impacts of Reynolds number on Sherwood number in simulation data for cigarette smoke have been indicated in the figure 7. The Sh number, representing the ratio of convective to diffusive mass transport, can be expressed as:

$$Sh = (h_m D / D_t) \tag{12}$$

Where the airway segment characteristic diameter is D . Thus, obtaining h_m , the respiratory coefficient of mass transfer is vital in forecasting the vapours regional deposition accurately. The coefficient of mass transfer in terms of non-dimensional Sh number is a function of Schmidt number (Sc) and Re number, traditionally. It was developed a set of generalized $Sh=f(Re, Sc)$ equations in respect to a model of human airway for flow rates of normal inspiratory by Zhang & Kleinstreuer [29]. However, they were partly idealized. It is noteworthy that these correlations are for constant flows and the values of realistic deposition could be deduced based on constant matching flows with corrections of time delay. The correlation curves of the $Sh-Re_{local}$ have been indicated in the figure 7. They were simulated for cigarette smoke vapor. Moreover, the convection contribution impact (Re -number) on mass transfer could be observed in the figure 7.

$Sh = 2.451 \left(Re \frac{D_a}{D_t} \right)^{0.325}$. The diameter of local equivalent computed is D_a as $D_a = \left(4A_L / \pi \right)^{1/2}$, where average cross-sectional area is A_L , the equivalent diameter of trachea is D_t , and $Re = 4flr / \pi \nu D_a$, where flr is the local flow rate at peak inspiration. Figure 7 shows the effects of Re number on Sh number in simulation data for cigarette smoke. The Re number increment results to increase in the nano-particles turbulent motion, on the other hand, the stronger the convection (Re numbers) is, the higher the mass transfer. Furthermore, the flow structures and airway geometric features influence a lot on cigarette smoke mass transport. Particularly, due to the interactions among local geometric features, flow turbulence and upstream deposition, the $Sh=Sh(Re)$ relationship may be different at various airway areas. The occurrence of upstream turbulent flows may affect both the inlet velocity and particle profiles which enter the bifurcation and could increase deposition within the model.

3. Conclusion

The mass transfer and deposition of cigarette smoke inside the human airway are investigated by the finite element method in this research. That is to say, the mass transfer and deposition of four selected tobacco-smoke vapors, acetaldehyde, acrolein, 1, 3-butadiene and carbon monoxide, in a human airway model under puffing as well as constant flow conditions have been simulated. The deposition of butadiene vapor and carbon monoxide gas is negligible in comparison to acrolein and acetaldehyde in the total human airways from mouth to generation B3. The deposition of particle decreased with increasing the diameter illustrated by the results. Moreover, the particle deposition decreased with the flowrate increment. The concentration profile of the airway edges was higher than the airway center. This distribution of concentration reduced slowly because of the nano-particle deposition in airway length apart from B3. Moreover, the results illustrate that deposition of cigarette smoking vapor in the upper airway is more than the lower airway. The results are likely to enhance assessing the level of cigarette-smoke damage in the total lung airway.

Nomenclature

v, u	Components of the velocity in the Cartesian coordinates ($m s^{-1}$)
P	Pressure (pa)
μ	Density of the cigarette smoke ($N s m^{-2}$)
ρ	Dynamic viscosity of the cigarette smoke ($kg m^{-3}$)

ω	Dissipation per unit turbulence kinetic energy (s^{-1})
k	Turbulence kinetic energy ($m^2 s^{-2}$)
τ	Reynolds stress tensor ($N m^{-2}$)
ϑ	Kinetic viscosity ($m^2 s^{-1}$)
A_i	Local wall cell area (m^2)
ϑ_T	Turbulent viscosity ($Ns m^{-2}$)
Sh	Sherwood number
Re	Reynolds number
k_B	Boltzmann constant ($1.38 \times 10^{-23} JK^{-1}$)
Y	Cigarette smoke concentration
DF	Deposition fraction (%)
\tilde{D}_p	Molecular diffusivity of cigarette smoke in air ($m^2 s^{-1}$)
\tilde{D}	Coefficient of aerosol diffusion ($m^2 s^{-1}$)
C_{slip}	Slip correction factor
λ_m	Mean free path (cm)
d_p	Diameter of droplet (nm)
T_w	Temperature at wall (K)
\dot{m}_w	Mass flux of local wall ($kg s^{-1}$)
L	Length (m)

References

- [1] World Health Organization Tobacco Free Initiative. Oslo, Norway: WHO Workshop on Advancing Knowledge on Regulating Tobacco Products, (2000). Retrieved from www.who.int/tobacco/media/en/OsloMonograph.pdf
- [2] A. Rodgman, T.A. Perfetti, The chemical components of tobacco and tobacco smoke, CRC press: Boca Raton. FL., USA, (2013).
- [3] J. Fowles, E. Dybing, Application of toxicological risk assessment principles to the chemical constituents of cigarette smoke, Tobacco Control. 12(4), 424–430, (2003)
- [4] US Food and Drug Administration, Harmful and potentially harmful constituents in tobacco products and tobacco smoke, Established list, (2012).
- [5] B.J. Ingebrethsen, Evolution of the particle size distribution of mainstream cigarette smoke during a puff, Aerosol science and technology, 5(4), 423–433, (1986).
- [6] B.J. Ingebrethsen, S.L. Alderman, B. Ademe, Coagulation of mainstream cigarette smoke in the mouth during puffing and inhalation, Aerosol science and technology, 45(12), 1422–1428, (2011).
- [7] G. Patskan, W. Reininghaus, Toxicological evaluation of an electrically heated cigarette. Part 1: Overview of technical concepts and summary of findings, Journal of Applied Toxicology: An International Journal., 23(5), 323–328, (2003).
- [8] T.R. Church, K.E. Anderson, N.E. Caporaso, M.S. Geisser, C.T. Le, Y. Zhang, A.R. Benoit, S.G.

- Carmella, SS. Hecht, A prospectively measured serum biomarker for a tobacco-specific carcinogen and lung cancer in smokers, *Cancer Epidemiology and Prevention Biomarkers*, 18(1), 260–266, (2009).
- [9] S. Lin, S. Fonteno, JH. Weng, P. Talbot, Comparison of the toxicity of smoke from conventional and harm reduction cigarettes using human embryonic stem cells, *Toxicological Sciences*, 118(1), 202–212, (2010).
- [10] Z. Zhang, C. Kleinstreuer, Airflow structures and nano-particle deposition in a human upper airway model, *Journal of computational physics.*, 198(1), 178–210, (2004).
- [11] M.E. Erdogan, C. Erdem İmrak, “An analytical solution of the Navier-stokes equation for flow over a moving plate bounded by two side walls,” *Strojniški vestnik*, 55(12), 749–754, (2009).
- [12] H.Y. Luo, Y. Liu, X.L. Yang, Particle deposition in obstructed airway, *Journal of Biomechanics*, 40(14), 3096-3104, (2007).
- [13] Z. Li, C. Kleinstreuer, Z. Zhang, Simulation of airflow fields and micro particle deposition in realistic human lung airway models. Part II: Particle transport and deposition, *European Journal of Mechanics-B/Fluids*, 26(5), 650-668, (2007).
- [14] H. Zhang, G. Papadakis, Computational analysis of flow structure and particle deposition in a singles asthmatic human airway bifurcation, *Journal of biomechanics*, 43(13), 2453-2499, (2010).
- [15] M. Khajenoori, A. Haghighi Asl, Heat and mass transfer simulation of the human airway for nano-particle water vapor, *Journal of Chemical Health and Safety*, 23(6), 33-39, (2016).
- [16] PMP. Data sets provided by Philip Morris Products S. A. (Neuchâtel, Switzerland), (2010).
- [17] Z. Zhang, C. Kleinstreuer, JF. Donohueand, CS. Kim, Comparison of micro- and nano-size particle depositions in a human upper airway model, *Journal of aerosol science*, 36(2), 211–233, (2005).
- [18] Y.G. Lv, J. Liu, J. Zhang, Theoretical evaluation of burns to the human respiratory tract due to inhalation of hot gas in the early stage of fire, *Burns*, 32(4), 436-446, (2006).
- [19] H. Moghadasa, O. Aboualia, A. Faramarzib, G. Ahmadi, Numerical investigation of sepal deviation effect on deposition of nano and micro particles in human nasal passage, *Respiratory physiology & neurobiology*, 177(1), 9–18, (2011).
- [20] S. Kongnuan, J. Pholuang, A Fourier series-based analytical solution for the oscillating airflow in a human respiratory tract, *International journal of pure and applied mathematics*, 78(5), 721–733, (2012).
- [21] Z. Zhang, C. Kleinstreuer, Low Reynolds number turbulent flows in locally constricted conduits: a comparison study, *AIAA Journal.*, 41(5), 831–840, (2003).
- [22] AEA Technology CFX-4.4: Solve, CFX International, Oxford shire, UK, (2001).
- [23] Z. Zhang, C. Kleinstreuer, Yu. Feng, Vapor deposition during cigarette smoke inhalation in a subject-specific human airway model, *Journal of Aerosol Science*, 53, 40–60, (2012).
- [24] A. Bejan, *Convection Heat Transfe*, John. Wiley & Sons. Inc., New York, (1995).
- [25] BJ. Fan, YS. Cheng, HC. Yeh, Gas collection efficiency and entrance flow effect of an annular diffusion denuder, *Aerosol Science and technology*, 25(2), 113–120, (1996).
- [26] DM. Bernstein, A review of the influence of particle size, puff volume, and inhalation pattern on the deposition of cigarette smoke particles in the respiratory tract, *Inhalation toxicology*, 16(10), 675–689, (2004).
- [27] Z. Zhang, C. Kleinstreuer, Deposition of naphthalene and tetradecane vapors in models of the human respiratory system, *Inhalation toxicology*, 23(1), 44–57, (2011).
- [28] D.D. McRae, The physical and chemical nature of tobacco smoke, *Recent Advances in tobacco science*, 16, 233–323, (1990).
- [29] R.R. Baker, M. Dixon, The retention of tobacco smoke constituents in the human respiratory tract, *Inhalation toxicology*, 18(4), 255–294, (2006).